ISBN: 978-3-95450-184-7 doi:10.18429/JACoW-IPAC2018-MOPMK016

CALCULATIONS OF BEAM-BEAM EFFECT AND LUMINOSITY FOR CRAB DYNAMICS SIMULATIONS IN JLEIC

He Huang†, Old Dominion University, Norfolk, VA 23529, U.S.A.
Vasiliy Morozov, Amy Sy, Jefferson Lab, Newport News, VA 23606, U.S.A.

Abstract

Crab crossing is an integral part of the Jefferson Lab Electron-Ion Collider (JLEIC) design to achieve high luminosity while meeting the detection and physics program requirements. The crab crossing scheme provides a head-on beam-beam collision for beams with a nonzero crossing angle. Simulations of crabbing dynamics currently do not include beam-beam effects. We describe a framework for accurate simulation of beam-beam effects on crabbing dynamics by applying a numerical calculation of the Bassetti-Erskine analytic solution to symplectic particle tracking codes. The numerical calculation is benchmarked against the analytic solution by calculating the luminosity reduction for several colliding beam scenarios. Benchmarking results show good agreement between the numerical calculation and analytic solution, paving the way for implementation of the beam-beam kick to Elegant tracking simulations.

MOTIVATION

As part of the strategy for achieving high luminosity, the Jefferson Lab Electron-Ion Collider (JLEIC) design requires high collision frequency and therefore fast separation of the colliding beams. Detection and physics program requirements impose additional constraints on the colliding beams such that the fast separation can only be achieved by colliding the beams at an angle. Collider luminosity formulas assume head-on collisions, thus giving the maximum luminosity for a given beam intensity. Without compensation of the crossing angle at the interaction point, the beams no longer collide head-on and the luminosity is reduced. The compensation is achieved by "crabbing," or tilting, each beam by half of the crossing angle such that the two beams collide head-on in the center of momentum frame. For the JLEIC design, a local crabbing scheme is used and thus each beam is crabbed before collision and de-crabbed after collision. Figure 1 shows a schematic of the crab crossing required to restore head-on collisions.

Current simulations of crabbing dynamics [1] in symplectic tracking codes such as Elegant do not include beam-beam effects that are important to understanding the full beam dynamics. We are implementing a beam-beam interaction model in Python that will interface to Elegant to accurately include beam-beam effects in the particle tracking simulations of crabbing dynamics. The simulation framework is as follows: The particle distribution is initiated at the start point of the tracking simulation. The beam is tracked through the first crab cavity and is transported to the interaction point. At the interaction point (IP), the particle distribution information is written out and fed into a Python script for applying the beam-beam interaction. The kicked distribution is fed back into Elegant for continued tracking through the second crab cavity and the rest of the collider ring optics. The simulation flow is illustrated in Fig. 2.

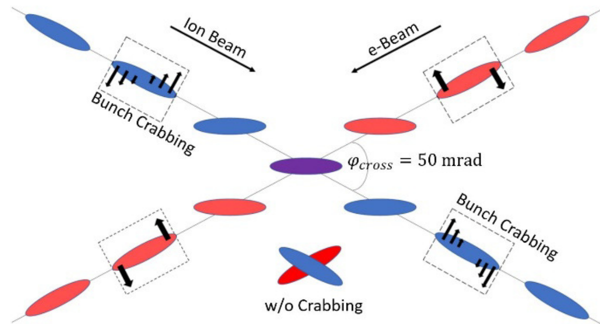

Figure 1: Schematic of local crabbing for JLEIC.

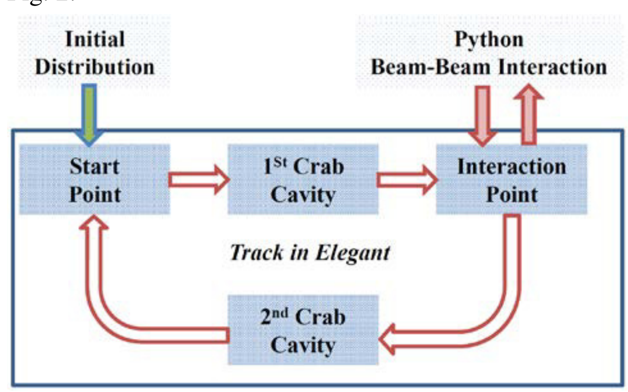

Figure 2: Simulation flow for beam-beam interaction.

The beam-beam interaction model is described in the following sections and is benchmarked against theoretical results by calculating the luminosity reduction for several colliding beam scenarios.

BEAM-BEAM INTERACTION MODEL

Our calculation model is based on the Bassetti-Erskine analytic solution [2] of the beam-beam interaction. It is extended to finite-length bunches using a symplectic algorithm proposed by Hirata [3, 4]. In this algorithm, each of the colliding finite-length bunches is split into multiple longitudinal slices. Then the beam-beam interaction reduces to consecutive pair-wise collisions of these thin slices. The algorithm calculates the longitudinal position of each collision and properly propagates the slice parameters to that point from the IP. The beam-beam kick is then applied to each particle in the slice using the Bassetti-Erskine

† huang@jlab.org

ISBN: 978-3-95450-184-7 doi:10.18429/JACoW-IPAC2018-MOPMK016

formula. At the same time, the luminosity can be calculated as a function of the beam sizes, crossing angle, transverse offsets, and hourglass effect.

We first simplify the luminosity calculation by transforming the coordinates to a Lorentz-boosted frame as in [3], where momenta of the bunches are purely longitudinal. The luminosity can be affected by the hourglass effect, bunch tilt about its center and its transverse offset. There are analytic solutions that allow for calculation of the luminosity reduction factor $\mathcal{L}/\mathcal{L}_0$ due to these effects, where $\mathcal{L}_0$ is the maximum luminosity.

For the symmetric-collider case, $\sigma_{1x}^* = \sigma_{2x}^*$, $\sigma_{1y}^* = \sigma_{2y}^*$, $\sigma_{1s} = \sigma_{1s}$, and for a flat beam, $\sigma_y^* \ll \sigma_x^*$. When including the hourglass effect, beam-tilt effects, and transverse offsets δ_x and δ_y, the luminosity reduction factor can be calculated with the following approximate solution [4],

$$\frac{\mathcal{L}}{\mathcal{L}_0} = \sqrt{\frac{2}{\pi}} a e^b K_0(b) \cdot \exp\left[-\frac{\left(\delta_x / 2\right)^2}{\sigma_x^{*2}\cos^2\phi + \sigma_z^{*2}\sin^2\phi} - \left(\frac{\delta_y}{2\sigma_y^*}\right)^2 \right] \quad (1)$$

where $K_0(b)$ is modified Bessel function of the Second kind and

$$a = \frac{\beta_y^*}{\sqrt{2}\sigma_z^*}, \quad b = a^2\left[1 + \left(\frac{\sigma_z^*}{\sigma_x^*}\tan\phi\right)^2\right]$$

NUMERICAL CALCULATION AND RESULTS

In a real collider ring, misalignments and magnetic imperfections may yield orbit distortions and then lead to a combination of crossing angle and beam offset effects.

In our numerical calculation processes, two colliding bunched beams are cut into many slices whose normal direction is parallel to the longitudinal direction. In the boosted frame, we obtained a more comprehensive formula for the numerical calculation. Including the hourglass effect [5], the beam-tilt effects and the beam offset effects, the luminosity is calculated by the summation of each individual discrete part.

$$\mathcal{L} = \frac{N_B f_c}{2\pi} \sum_{i,j} \mathcal{L}_{0_{i,j}} \mathcal{A}_{i,j} O_{i,j} C_{i,j} \quad (2)$$

where N_B is the number of colliding bunches; f_c is the collision frequency;

$$\mathcal{L}_{0_{i,j}} = \frac{N_{1,i} N_{2,j}}{\sqrt{\sigma_{x1,i}^2 + \sigma_{x2,j}^2}\sqrt{\sigma_{y1,i}^2 + \sigma_{y2.j}^2}}$$

$$\mathcal{A}_{i,j} = \frac{1}{\sqrt{1 + \frac{\sigma_{1z}^2 + \sigma_{2z}^2}{\sigma_{x1,i}^2 + \sigma_{x2,j}^2}\tan^2\phi_x + \frac{\sigma_{1z}^2 + \sigma_{2z}^2}{\sigma_{y1,i}^2 + \sigma_{y2,j}^2}\tan^2\phi_y}}$$

$$O_{i,j} = \exp\left[-\frac{\delta_x^2}{2\left(\sigma_{x1,i}^2 + \sigma_{x2,j}^2\right)} - \frac{\delta_y^2}{2\left(\sigma_{y1,i}^2 + \sigma_{y2,j}^2\right)} \right]$$

$$C_{i,j} = \exp\left[\mathcal{A}^2 \frac{\sigma_{1z}^2 + \sigma_{2z}^2}{2} \left(\frac{\delta_x \tan\phi_x}{\sigma_{x1,i}^2 + \sigma_{x2,j}^2} + \frac{\delta_y \tan\phi_y}{\sigma_{y1,i}^2 + \sigma_{y2,j}^2} \right)^2 \right]$$

For Eq. (2), $\mathcal{L}_{0_{i,j}}$ is the luminosity for two head-on slices. The reduction factor $\mathcal{A}_{i,j}$ describes the effect of two different crossing angles. The factor $O_{i,j}$ describes the reduction due to offsets of the beam slices. If both the tilt effect and offset effect exist simultaneously, the coupling reduction effect, $C_{i,j}$, is less than unity in the luminosity calculation.

We compared the numerical calculations to the analytic solution for different colliding beam scenarios. In benchmarking the analytic solution, the following parameters were used: symmetric-electron-collider; flat beam, $\sigma_x = 50\sigma_y$; one crossing angle and one offset; electron beam energy 10.0 GeV; collision frequency 1.18×10^8 Hz; number of electrons for each beam is 3.7×10^{10}; normalized emittance $\varepsilon_{nx} = 4.32 \times 10^{-2}$. The luminosity is given in units of $cm^{-2}s^{-1}$. Table 1 lists the parameters used for the numerical calculations.

Table 1: Parameters for Cases 1−4

Parameter	Case 1	Case 2	Case 3	Case 4
σ_z (cm)	1.0	1.0	0.1~1.0	10.0
ε_{Ny} (cm)	1.72	1.72	1.72	1.72
β_x^* (cm, 10^{-5})	400.0	4.0	4.0	4.0
β_y^* (cm, 10^{-5})	80.0	0.8	0.8	0.8
ϕ_x (mrad)	0~105	0~105	0	0
δ_x (unit: σ_x)	0	0	0	0~3
Slices/Bunch	10	20	1~100	10

Case 1: *Flat beams, no hourglass effect, with offset*. Because $\sigma_z \ll \beta_x^*$ and $\sigma_z \ll \beta_y^*$, the hourglass effect is not significant; for example, when "head-on"(ϕ_x=0), the luminosity reduction factor is 1. The major reduction of the luminosity comes from the crossing angle. Figure 3 shows the numerical result matches the analytic result very well.

Case 2: *Flat beams, with hourglass effect, no offset*. For this case, $\beta_{1x}^* = \beta_{2x}^* = \beta_x^*$. Both the analytic and numerical results demonstrate the hourglass effect in Fig. 4.

Case 3: *Head-on flat beams, with hourglass effect, no offset*. We choose $\beta_{1x}^* = \beta_{2x}^* = \beta_x^*$ and $\beta_{1y}^* = \beta_{2y}^* = \beta_y^*$. In Fig. 5, with increasing number of electron bunch slices and increasing bunch length, the hourglass effect becomes more apparent. The two solutions begin to diverge because

ISBN: 978-3-95450-184-7 doi:10.18429/JACoW-IPAC2018-MOPMK016

the analytic solution is an approximate result, and the beams are not sufficiently flat to satisfy the $\sigma_y^* \ll \sigma_x^*$ condition for which the analytic result is valid.

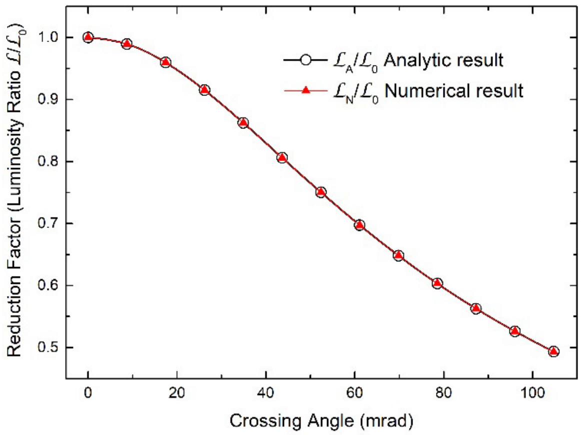

Figure 3: Numerical calculation vs. analytic result for the case with flat beams, no hourglass effect, with offset.

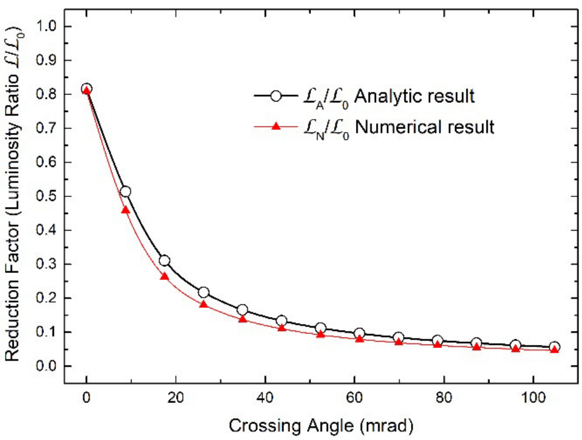

Figure 4: Numerical calculation vs. analytic solution for the case with flat beams, hourglass effect, and no offset.

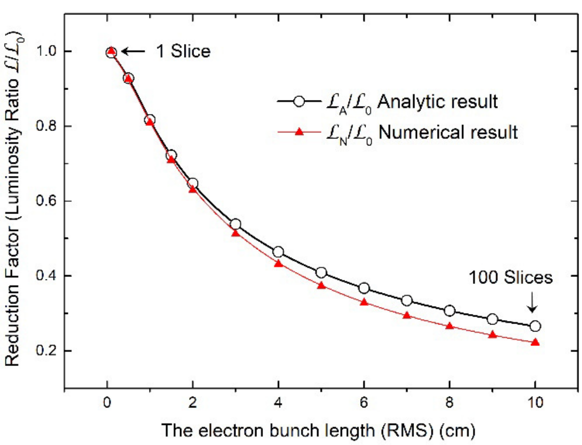

Figure 5: Numerical calculation vs. analytic solution for head-on flat beams, hourglass effect, and no offset.

Case 4: *Head-on flat beams, with hourglass effect, with transverse offset*. Figure 6 plots the luminosity reduction factor as a function of transverse offset.

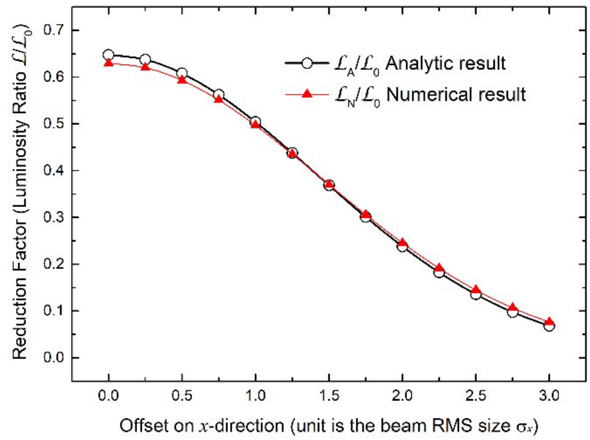

Figure 6: Numerical calculation vs. analytic result for head-on flat beams, with hourglass effect, with varying offset.

Case 5:*Head-on collision with Hourglass Effect for JLEIC.* For JLEIC simulation parameters (see Table 2) with the collision frequency 1.19×10^8 Hz, finally we obtain the luminosity of JLEIC design is 5.75×10^{33} cm^{-2}/s, the hourglass reduction factor is 0.75.

Table 2: Parameters in Case 5

Parameter	Electron	Electron
Beam Energy (GeV)	100	100
σ_z (cm)	2.2	1.0
ε_N , hor / ver, (cm, 10^{-4})	0.9/0.18	432/86.4
β^* , hor / ver, (cm)	10.5/2.1	4.0/0.8
Particles/Bunch (10^{10})	3.9	3.7
Slices/Bunch	22	10

FUTURE PLANS

We next plan to interface our beam-beam and luminosity calculation code to Elegant models of the JLEIC collider rings. This will combine Elegant's accurate simulation of the beam dynamics in the collider lattice with a somewhat simplified but sufficiently accurate beam-beam interaction model that captures the main physical features of the process. The beam parameters used in our code will be extracted from the tracking data. The Bassetti-Erskine kick will then be applied to individual particles and the resulting beam distribution will be used in Elegant simulation. We will then study various aspects of the crabbing dynamics with beam-beam effect using luminosity evolution as one of the performance criteria. We will also benchmark our simulation results using other beam-beam codes such as GHOST [6] and Beambeam3D [7].

ACKNOWLEDGMENTS

This material is based upon work supported by the U.S. Department of Energy, Office of Science, Office of Nuclear Physics under contracts DE-AC05-06OR23177 and DE-AC02-06CH11357.

ISBN: 978-3-95450-184-7 doi:10.18429/JACoW-IPAC2018-MOPMK016

REFERENCES

[1] S. Sosa, V. S. Morozov, and J. R. Delayen, "Modeling Local Crabbing Dynamics in the JLEIC Ion Collider Ring," in *Proc. IPAC2017*, Copenhagen, Denmark, May 2017, paper WEPIK043, pp. 3022-3024.

[2] M. Bassetti and G. Erskine, "Closed Expression for the Electrical Field of A Two-Dimensional Gaussian Charge," Tech. Rep., CERN-ISRTH/80-06, 1980.

[3] K. Hirata, "Analysis of Beam-Beam Interactions with a Large Crossing Angle," *Phy. Rev. Lett.*, vol. 74, p. 2228, May 1995.

[4] A. W. Chao, "Operational Considerations," in *Handbook of Accelerator Physics and Engineering*, 3rd Printing, World Scientific Publishing Co. Pte. Ltd. 2009, pp. 278-279.

[5] M. A. Furman, "Hourglass Effects for Asymmetric Colliders," *Proceedings of the IEEE Particle Accelerator Conference*, San Francisco, CA, May 1991, pp. 422-424.

[6] B. Terzic *et al.*, "High-Fidelity Simulation of Long-Term Beam-Beam Dynamics on GPUs," in *Proc. of ICAP2015*, Shanghai, China, Oct. 2015, paper TUCBC3, pp. 40-43.

[7] J. Qiang, R. Ryne and M. Furman, "Strong-Strong Beam-Beam Simulation Using a Green Function Approach," *Phys. Rev. ST Accel. Beams*, vol. 5, p. 104402, 2002.